Energy-time entanglement generation in optical fibers under CW pumping

Shuai Dong,[1] Qiang Zhou,[1] Wei Zhang,[1,*] Yuhao He,[2] Weijun Zhang,[2] Lixing You,[2] Yidong Huang,[1] and Jiangde Peng[1]

[1]*Tsinghua National Laboratory for Information Science and Technology, Department of Electronic Engineering, Tsinghua University, Beijing, 100084, China*
[2]*State Key Laboratory of Functional Materials for Informatics, Shanghai Institute of Microsystem and Information Technology, Chinese Academy of Sciences, Shanghai 200050, China*
[*]*zwei@tsinghua.edu.cn*

Abstract: In this paper, the energy-time entangled photon-pairs at 1.5 μm are generated by the spontaneous four wave mixing (SFWM) in optical fibers under continuous wave (CW) pumping. The energy-time entanglement property is demonstrated experimentally through an experiment of Franson-type interference. Although the generation rates of the noise photons are one order of magnitude higher than that of the photon-pairs under CW pumping, the impact of noise photons can be highly suppressed in the measurement by a narrow time domain filter supported by superconducting nanowire single photon detectors with low timing jitters and time correlated single photon counting (TCSPC) module with high time resolution. The experiment results show that the SFWM in optical fibers under CW pumping provides a simple and practical way to generate energy-time entanglement at 1.5 μm, which has great potential for long-distance quantum information applications over optical fibers.

OCIS codes: (270.0270) Quantum optics; (190.4370) Nonlinear optics, fibers; (190.4410) Nonlinear optics, parametric processes.

References and links

1. W. Tittel, J. Brendel, H. Zbinden, and N. Gisin, "Quantum cryptography using entangled photons in energy-time bell states," Phys. Rev. Lett. **84**, 4737 (2000).
2. I. Marcikic, H. De Riedmatten, W. Tittel, H. Zbinden, and N. Gisin, "Long-distance teleportation of qubits at telecommunication wavelengths," Nature (London) **421**, 509–513 (2003).
3. I. Ali-Khan, C. J. Broadbent, and J. C. Howell, "Large-alphabet quantum key distribution using energy-time entangled bipartite states," Phys. Rev. Lett. **98**, 060503 (2007).
4. Q. Zhang, H. Takesue, S. W. Nam, C. Langrock, X. Xie, B. Baek, M. Fejer, and Y. Yamamoto, "Distribution of time-energy entanglement over 100 km fiber using superconducting singlephoton detectors," Opt. Express **16**, 5776–5781 (2008).
5. V. Giovannetti, S. Lloyd, and L. Maccone, "Positioning and clock synchronization through entanglement," Phys. Rev. A **65**, 022309 (2002).
6. W. Tittel, J. Brendel, N. Gisin, and H. Zbinden, "Long-distance bell-type tests using energy-time entangled photons," Phys. Rev. A **59**, 4150 (1999).
7. L. Wang, C. Hong, and S. Friberg, "Generation of correlated photons via four-wave mixing in optical fibres," J. Opt. B: Quantum and Semiclass. Opt. **3**, 346 (2001).
8. M. Fiorentino, P. L. Voss, J. E. Sharping, and P. Kumar, "All-fiber photon-pair source for quantum communication," IEEE Photon. Technol. Lett. **27**, 491C493 (2002)
9. E. Brainis, "Four-photon scattering in birefringent fibers," Phys. Rev. A **79**, 023840 (2009).

#199979 - $15.00 USD Received 28 Oct 2013; revised 12 Dec 2013; accepted 17 Dec 2013; published 2 Jan 2014

10. M. Halder, J. Fulconis, B. Cemlyn, A. Clark, C. Xiong, W. J. Wadsworth, and J. G. Rarity,"Nonclassical 2-photon interference with separate intrinsically narrowband fibre sources," Opt. Express **17**, 4670–4676 (2009)
11. J. E. Sharping, M. Fiorentino, and P. Kumar, "Observation of twin-beam-type quantum correlation in optical fiber," Opt. Lett. **26**, 367–369 (2001).
12. K. Inoue and K. Shimizu, "Generation of quantum-correlated photon pairs in optical fiber: influence of spontaneous raman scattering," Jpn. J. Appl. Phys. **43**, 8048 (2004).
13. X. Li, J. Chen, P. Voss, J. Sharping, and P. Kumar, "All-fiber photon-pair source for quantum communications: Improved generation of correlated photons," Opt. Express **12**, 3737–3744 (2004).
14. H. Takesue and K. Inoue, "1.5-μm band quantum-correlated photon pair generation in dispersion-shifted fiber: suppression of noise photons by cooling fiber," Opt. Express **13**, 7832–7839 (2005).
15. Q. Zhou, W. Zhang, J. Cheng, Y. Huang, and J. Peng, "Polarization-entangled bell states generation based on birefringence in high nonlinear microstructure fiber at 1.5 μm," Opt. Lett. **34**, 2706–2708 (2009).
16. Q. Zhou, W. Zhang, J. Cheng, Y. Huang, and J. Peng, "Noise performance comparison of 1.5 μm correlated photon pair generation in different fibers," Opt. Express **18**, 17114–17123 (2010).
17. B. Fang, O. Cohen, J. B. Moreno, and V. O. Lorenz, "State engineering of photon pairs produced through dual-pump spontaneous four-wave mixing," Opt. Express **21**, 2707–2717 (2013).
18. Q. Zhang, X. Xie, H. Takesue, S. W. Nam, C. Langrock, M. M. Fejer, and Y. Yamamoto, "Correlated photon-pair generation in reverse-proton-exchange PPLN waveguides with integrated mode demultiplexer at 10 GHz clock," Opt. Express **15**, 10288-10293 (2007)
19. J. Franson, "Bell inequality for position and time," Phys. Rev. Lett. **62**, 2205–2208 (1989).
20. J. S. Bell, "On the einstein-podolsky-rosen paradox," Physics **1**, 195–200 (1964).
21. J. F. Clauser, M. A. Horne, A. Shimony, and R. A. Holt, "Proposed experiment to test local hidden-variable theories," Phys. Rev. Lett. **23**, 880–884 (1969).
22. L. You, X. Yang, Y. He, W. Zhang, D. Liu, W. Zhang, L. Zhang, L. Zhang, X. Liu, S. Chen, Z. Wang, and X.Xie, "Jitter analysis of a superconducting nanowire single photon detector," AIP Advances **3**, 072135 (2013).
23. S. Chen, D. Liu, W. Zhang, L. You, Y. He, W. Zhang, X. Yang, G. Wu, M. Ren, H. Zeng, Z. Wang, X. Xie, and M. Jiang, "Time-of-flight laser ranging and imaging at 1550 nm using low-jitter superconducting nanowire single-photon detection system," Applied optics **52**, 3241–3245 (2013).
24. J. Pan, Z. Chen, C. Lu, H. Weinfurter, A. Zeilinger, and M. Żukowski, "Multiphoton entanglement and interferometry," Rev. Mod. Phys. **84**, 777 (2012).
25. H. de Riedmatten, I. Marcikic, V. Scarani, W. Tittel, H. Zbinden, and N. Gisin, "Tailoring photonic entanglement in high-dimensional hilbert spaces," Phys. Rev. A **69**, 050304 (2004).

1. Introduction

As an entanglement resource robust to environment variation, energy-time entanglement of photons has been used to realize many quantum information applications such as quantum communication [1–4] and quantum clock synchronization [5]. Traditionally, energy-time entangled photon-pairs are realized via spontaneous parametric down conversion (SPDC) in nonlinear crystals [1–3] or periodically poled lithium niobate (PPLN) [4]. By this scheme, the properties of energy-time entanglement have been widely investigated and many applications have been developed [1–4, 6]. Recently, the development of long distance quantum information applications over optical fibers requires energy-time entangled photon-pairs at 1.5 μm. A promising way to realize it is based on the spontaneous four wave mixing (SFWM) process in nonlinear optical fibers [7–17]. During the SFWM process in optical fibers, two pump photons are annihilated, while two photons are generated simultaneously. The energy conservation in the SFWM process ensures that there is energy-time entanglement between the generated two photons. However, in the experimental realization of this scheme, noise photons without energy-time entanglement are unavoidable. The noise photons are mainly generated by the spontaneous Raman scattering when pump light propagates through the optical fiber, if the pump light is filtered out sufficiently. Previous work has shown that since the generation rate of the entangled photon-pairs is proportional to the square of the pump power, while, that of the noise photons is proportional to the pump power, pulsed pump light with high peak power and narrow pulse width is preferred to realize correlated photon-pairs generation with low noise [12–16]. On the contrary, continuous wave (CW) pumping scheme is regarded as difficult since the generation rates of noise photons mainly via spontaneous Raman scattering process would be far higher

#199979 - $15.00 USD Received 28 Oct 2013; revised 12 Dec 2013; accepted 17 Dec 2013; published 2 Jan 2014

than that of entangled photon-pairs, which would destroy the energy-time entanglement.

Time domain filter is a measurement technique to select the correlated photons in time domain [2]. Previous works have shown that it is an effective method to increase the signal to noise ratio in coincidence count measurement of correlated photon pairs [4, 18]. Since in these works the entangled photon pairs were generated by SPDC in PPLN with little noise photons, the narrow time domain filters were used to suppress the impact of dark counts of single photon detectors. In this paper, time domain filter is used to suppress the impact of high-level noise photons by the spontaneous Raman scattering process in the experiment of energy-time entangled photon-pairs generation in optical fiber under CW pumping. Theoretical analysis shows that the time domain filter can select out the contribution of entangled photon-pairs from the coincidence count under high noise level and improve the signal to noise ratio. In the experiment, superconducting nanowire single photon detectors (SNSPDs) and high resolution time correlated single photon counting (TCSPC) module are used to measure the coincidence count of the photons generated. The low timing jitters of the SNSPDs and the high time-resolution of the TCSPC module ensure that narrow time domain filter can be realized to suppress the noise photons effectively and make it possible to explore the energy-time entanglement between the signal and idler photons. The energy-time entanglement is demonstrated by an experiment of Franson-type interference [19] and a violation of CHSH-Bell inequality [6, 20, 21] is presented, showing that the SFWM in optical fibers under CW pumping provides a simple way to realize energy-time entangled photon pairs at 1.5 μm, which would have great potential in long-distance quantum information applications over optical fibers.

2. Photon-pairs generation in optical fibers under CW pumping

In the photon-pairs generated by the SFWM process in optical fibers, the photon with a frequency higher than that of the pump light is named as signal photon, while, the other photon is named as idler photon, with a frequency lower than that of the pump light. The frequencies of the pump light, signal photon and idler photon, denoted by ω_p, ω_s and ω_i respectively, satisfy the relation of $\omega_s + \omega_i = 2\omega_p$, which is determined by the energy conservation in the SFWM process. On the other hand, noise photons are also generated at both signal and idler sides mainly due to the spontaneous Raman scattering. In experiments, the photons at both sides are filtered out and detected by single photon detectors, respectively. The count rates at signal and idler sides (denoted by C_s and C_i, respectively) can be expressed as [14, 15]

$$C_s = \eta_s R + \eta_s R_s + D_s \quad (1)$$

$$C_i = \eta_i R + \eta_i R_i + D_i \quad (2)$$

where, R is the generation rate of the entangled photon-pairs, R_s and R_i are generation rates of the noise photons, η_s and η_i are the collection and detection efficiencies of photons, D_s and D_i are dark count rates of the single photon detectors at signal and idler sides, respectively.

The measurement of TCSPC is an effective way to demonstrate the energy-time entangled photon-pairs generation under CW pumping. In this measurement, the output of one detector (e.g. signal side detector) is used as the trigger to start the timer in TCSPC to record the relative time of the output of the other detector (e.g. the idler side detector). After a period of time, the recorded start-stop events are classified on the discrete time space (time bins) according to the time between the two photons and the number of events at each time bin is recorded. For most of the time bins, the photons at signal side and idler side are independent with each other, hence, the count rates for these time bins are named as accidental coincidence count and can be expressed as

$$C_a = C_s C_i \tau \quad (3)$$

#199979 - $15.00 USD Received 28 Oct 2013; revised 12 Dec 2013; accepted 17 Dec 2013; published 2 Jan 2014

where τ is the width of the time bin. However, there is a special time bin with significantly higher count, in which the photon pairs generated by the SFWM in optical fibers are recorded. The count rate for this time bin is called coincidence count rate and can be expressed as

$$C_c = \eta_s \eta_i R + C_a \tag{4}$$

In the case of SFWM process in optical fibers under CW pumping, usually R_s and R_i is far higher than R and D_i, D_s. Hence, accidental coincidence count Eq. (3) can be simplified under high noise level,

$$C_a \approx \eta_s \eta_i R_s R_i \tau + \eta_s \eta_i R (R_s + R_i) \tau \tag{5}$$

It can be seen that most terms in Eq. (5) are related to the time bin width τ while the coincidence count rate caused by photon-pairs generated via SFWM is not. The coincidence count to accidental coincidence count ratio (CAR) can be expressed as

$$\mathrm{CAR} = \frac{C_c}{C_a} \approx \frac{R}{[R_s R_i + R(R_s + R_i)]\,\tau} + 1 \tag{6}$$

It can be seen that even with high noise level, a high CAR can be achieved if the time bin is sufficiently narrow. The specific time bin acts as a time domain filter to reduce the impact of the noise photons based on the generation simultaneity of the two photons in a photon-pair via SFWM. It provides a simple way to realize high performance energy-time entanglement measurement under high noise level.

It is worth to note that in the experiment, the coincidence count may spread to many time bins due to the coherence time of the photons, the timing jitters of the single photon detectors, and time resolution of the TCSPC module. Contributions of all these bins should take into account, equivalent to apply a time domain filter with a width equal to the total of these bins. Hence, the width of the time domain filter is limited by the time-correlated properties of the photon pairs and measurement system. In the experiment shown in this paper, the time domain filter width is mainly decided by the timing jitters of the single photon detectors. The timing jitters of SNSPDs are far smaller than that of traditional single photon detectors based on InP/InGaAsP avalanche photodiodes (APDs) at 1.5 μm [22, 23], hence, they could support a narrower time domain filter to reduce the impact of noise photons. In the following, SNSPDs are used to demonstrate energy-time entanglement generation via the SFWM process in optical fibers under CW pumping experimentally.

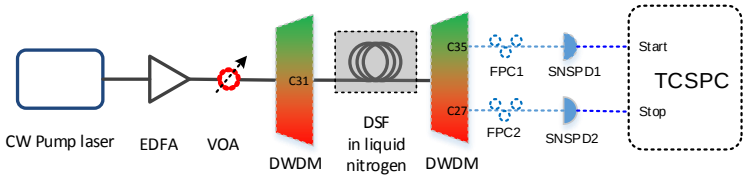

Fig. 1. Experiment setup. A CW laser was used as the pump light source; EDFA: erbium doped fiber amplifier; VOA: variable optical attenuator; DWDM: dense wavelength division multiplexing device; FPC: fiber polarization controller; SNSPD: superconducting nanowire single photon detector; TCSPC: time correlated single photon counting module.

The experiment setup is shown in Fig. 1. CW pump light with a wavelength of 1552.16 nm (close to the center wavelength of ITU C31 channel, 1552.52 nm) was generated by a tunable laser (Agilent 81980A) and amplified by an erbium doped fiber amplifier (EDFA). The

#199979 - $15.00 USD Received 28 Oct 2013; revised 12 Dec 2013; accepted 17 Dec 2013; published 2 Jan 2014

linewidth of the tunable laser is 100 kHz. Cascaded DWDM devices were used as the pump filter to suppress the ASE noise of the EDFA. Then the pump light was injected into a piece of commercial dispersion shifted fiber (DSF). The length of the DSF was 500 meters and the zero dispersion wavelength was $\lambda_0 = 1549$ nm. The noise photons generated by spontaneous Raman scattering in the DSF were suppressed by cooling the fiber with liquid nitrogen bath [14]. At the output end of the DSF, a filter system made up of commercial DWDM devices was used to separate generated signal photons, idler photons and residual pump light. The residual pump light was used to monitor the pump power (not shown in Fig. 1 for simplicity). The center wavelengths of the signal photons and idler photons were 1555.75 nm (ITU C27 channel) and 1549.32 nm (ITU C35 channel), respectively, with a full width at half maximum (FWHM) of 139 GHz for idler photons and 118 GHz for signal photons. The total loss of the filtering system are about 3 dB at both sides. After the filter system, the signal and idler photons were directed to two NbN SNSPDs operated at 2.2 K in Gifford-Mcmahon cryocooler. The detection efficiencies and timing jitters of SNSPD1 and SNSPD2 are 4%, 40 ps and 2%, 20 ps respectively. The dark count rates were 30 Hz for both of them. Since the efficiencies of SNSPDs were polarization dependent, two fiber polarization controllers (FPCs) were used to adjust the polarization of photons before the two SNSPDs. A TCSPC module (picoharp300, picoQuant GmbH) was used to record the arrival time of photons at signal and idler sides and realize single side photon counting and coincidence count measurement. Its minimum time bin width is 4 ps and electrical time resolution is < 12 ps rms.

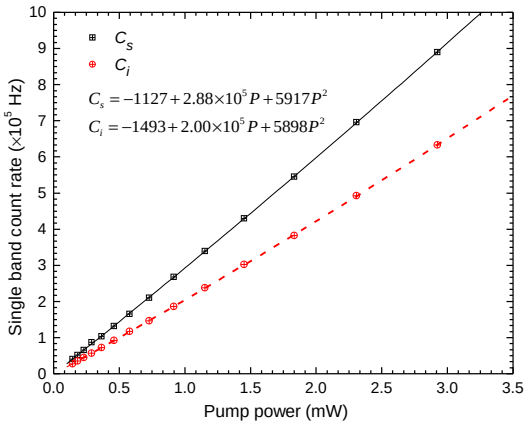

Fig. 2. Single side photon count rates. Squares and circles were results of signal and idler photons, respectively. The curve-fitting results are shown in the figure.

Figure 2 shows the experiment results of the single side photon count rates. The squares and circles are results of signal and idler photons, respectively. The dashed and solid lines are their fitting curves by the quadratic polynomials $C_{s,i} = a_{s,i}P^2 + b_{s,i}P + C_{0s,i}$. The fitting results are shown in Fig. 2. It can be seen that the count rates rise almost linearly under increasing pump levels at both sides, indicating that the noise photons generated by spontaneous Raman scattering are dominant at both sides.

The coincidence count results are shown in Fig. 3. In the measurement, the outputs of SNSPD1 and SNSPD2 were connected to the trigger and signal ports of the TCSPC module, respectively. Figure 3(a) shows the measured histogram of the coincidence count with a pump power of 2.92 mW. The histogram was the accumulation of coincidence events in 20 seconds. The time bin width of the TCSPC module was set to 4 ps. It can be seen that on the histogram,

#199979 - $15.00 USD Received 28 Oct 2013; revised 12 Dec 2013; accepted 17 Dec 2013; published 2 Jan 2014

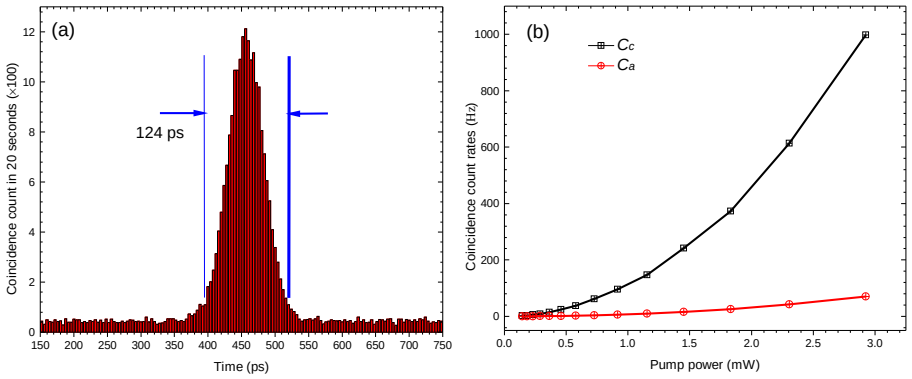

Fig. 3. Measurement results of coincidence count. (a) Typical experimental result of the coincidence count when the pump power is 2.92 mW. (b) Coincidence count rates and accidental coincidence count rates under different pump levels.

there is a coincidence peak on the background of accidental coincidence count because of the generation simultaneity of the two photons in a photon-pair via SFWM. The full width at half maximum (FWHM) of the coincidence peak is about 65 ps, which is decided by the timing jitters of the two SNSPDs, the time-resolution of the TCSPC module, and the filter bandwidth for signal and idler photons. The total coincidence count is calculated by the sum of the contributions of 31 time bins covering the coincidence peak, while the accidental coincidence count is estimated by the sum of 31 time bins outside the coincidence peak. Hence, the width of the equivalent time domain filter is 124 ps, the total time of 31 time bins. Figure 3(b) shows the measured C_c and C_a under different pump levels. It can be seen that the coincidence count rates are much larger than the accidental coincidence count rates for the sake of time domain filter, indicating that the impact of noise photons is effectively suppressed.

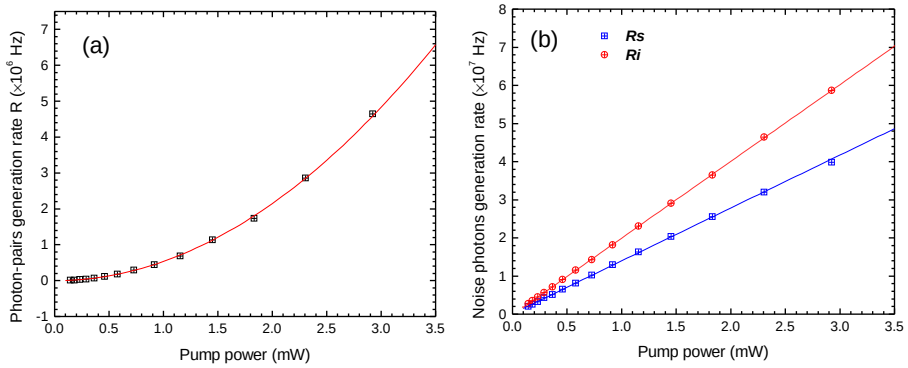

Fig. 4. Calculated results of R, R_s and R_i under different pump levels. (a) R under different pump levels: squares are calculated results, the red line is the fitting curve of $R = 5.38 \times 10^5 P^2$. (b) R_s and R_i under different pump levels. Squares and circles are calculated results, blue solid and red dashed lines are fitting curves of $R_s = 1.38 \times 10^7 P$, $R_i = 2.00 \times 10^7 P$.

According to the single side count measurement results in Fig. 2 and the coincidence count results in Fig. 3(b), the generation rates of photon-pairs and noise photons at signal side and idler side, i.e. R, R_s and R_i, can be calculated by solving the equation group of Eqs. (1),(2),(3), and (4), under different pump levels. In the calculation, the collection and detection efficiencies

#199979 - $15.00 USD Received 28 Oct 2013; revised 12 Dec 2013; accepted 17 Dec 2013; published 2 Jan 2014

are $\eta_s = 2\%$ and $\eta_i = 1\%$, the dark count rates of the two SNSPDs are $D_s = D_i = 30$ Hz according to the performances of the SNSPDs. The calculation results are shown in Fig 4. Figure 4(a) shows the results of R under different pump levels, in which the squares are the calculation results and the line is the fitting curve using $R = aP^2$ and $a = 5.38 \times 10^5$. It shows that R rises quadratically with increasing pump power. Figure 4(b) is the results of R_s and R_i, in which the squares and the circles are the calculated results, respectively, and the lines are their fitting curves using $R_{s,i} = b_{s,i}P$ and $b_s = 1.38 \times 10^7$, $b_i = 2.00 \times 10^7$, respectively. It shows that both R_s and R_i rise linearly with increasing pump power. These results agree well with the theoretical analysis of photon-pairs generated by SFWM in optical fibers [7, 13]. Comparing the results shown in Fig. 4, it can be seen that R_s and R_i are at least one order of magnitude higher than R under most pump levels in the experiment, showing the high noise property in the experiment of photon-pairs generation in optical fibers under CW pumping.

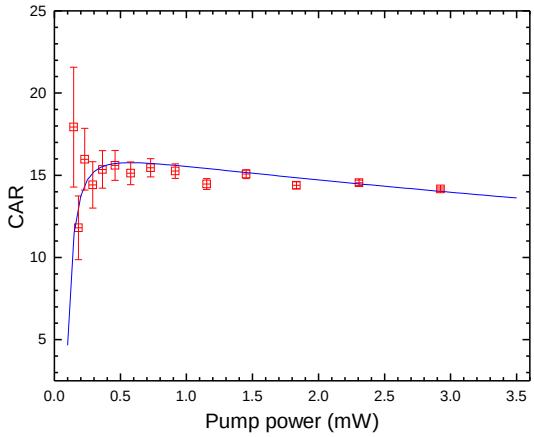

Fig. 5. CARs under different pump levels. The red squares are measured results. The blue line is the calculated result according to Eq. (6) utilizing the fitting curves shown in Fig. 4.

Although the noise level is very high, by the coincidence measurement and time domain filter, the impact of noise photons is suppressed effectively as shown in Fig. 3(b), in which C_c is far higher than C_a under different pump levels. The noise property of the energy-time entanglement can be presented directly by the CARs under different pump levels [13], which are shown in Fig. 5. The squares are the measurement results according to CAR $= C_c/C_a$ and the blue line is the calculated results according to Eq. (6) and the fitting curves in Fig. 4. It can be seen that CARs rise with decreasing pump at high pump levels, while, reduce rapidly when the pump levels are low. The maximum CAR is up to 15.8 under a pump level of 0.5 mW, indicating the impact of noise photons has been suppressed effectively in the energy-time entanglement measurement via time domain filtering.

3. Experiments of quantum interference and the violation of CHSH-Bell inequality

To demonstrate the energy-time entanglement in the photon-pairs generated via SFWM in optical fibers under CW pumping, experiments of the Franson-type interference [19] were performed based on this energy-time entanglement source and two unbalanced Mach-Zehnder interferometers (UMZIs), and a violation of CHSH-Bell inequality [6, 20, 21] was presented.

The experimental setup is shown in Fig. 6(a). The entangled photon-pairs were generated by the scheme in section 2. A commercial 10 GHz differential quadrature phase shift keying (DQPSK) demodulator (Optoplex Corp., DI-CAKFASO15-R1) was used as two independent

#199979 - $15.00 USD Received 28 Oct 2013; revised 12 Dec 2013; accepted 17 Dec 2013; published 2 Jan 2014

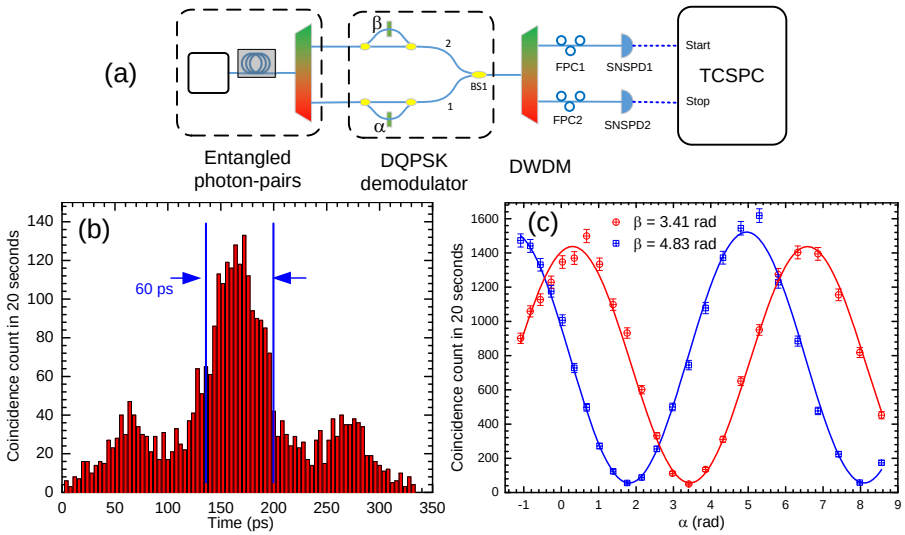

Fig. 6. Quantum interference of energy-time entanglement generated in the optical fiber under CW pumping. (a)Experimental setup. Photon pairs are generated in optical fibers under CW pumping, two UMZIs are realized utilizing a commercial 10 GHz DQPSK demodulator. α and β are the additional phases in the long arms of the two UMZI, respectively. An additional filter system for the signal and idler photons is used to get rid of the impact of the beam splitter (BS1) combining the two UMZIs in the DQPSK. (b) A typical result of the coincidence measurement and the applied time domain filter. (c) The measured interference fringes of the coincidence counts when changing α under $\beta = 3.41$ rad and $\beta = 4.83$ rad.

UMZIs. One more filter system made up of DWDM devices for the signal and idler photons is used to get rid of the impact of the beam splitter (BS1) combining the two UMZIs in the DQPSK. The optical path difference between the two arms of the UMZI was $\Delta t = 100$ ps. It is much less than the coherence time of the pump light ($T_c \sim 10$ μs, estimated by the linewidth of the pump light) and larger than that of single photons at each side (~ 7 ps, estimated by the filter bandwidth for the signal and idler photons). The additional phases in long arms of the two UMZIs are denoted by α and β, which can be adjusted by the applied voltages independently. The relations of the additional phases and the applied voltages of the two UMZIs are collimated before the experiment. The generated signal and idler photons were injected into the two UMZIs respectively, then they were detected by the SNSPDs and the coincidence count measurement was carried out.

Figure 6(b) shows a typical measured histogram. It can be seen that three coincidence peaks appear. The two lower peaks are contributions of coincidence counts that one photon passed through the long arm of one UMZI, while the other photon passed through the short arm of the other UMZI. The center peak is the contributions of coincidence counts that both photons pass through the long arms or the short arms of their corresponding UMZIs. The two-photon state of the signal and idler photons contributing to the center coincidence counts can be expressed as [24]

$$|\Phi\rangle = \frac{1}{\sqrt{2}}\left[|\text{short}\rangle_s|\text{short}\rangle_i + \exp\left(i(\alpha+\beta)\right)|\text{long}\rangle_s|\text{long}\rangle_i\right] \tag{7}$$

where, “short” and “long” represent the short and long arms through which the two photons passed. The former and latter terms in (7) are indistinguishable, hence, two-photon interference

#199979 - $15.00 USD Received 28 Oct 2013; revised 12 Dec 2013; accepted 17 Dec 2013; published 2 Jan 2014

fringes can be observed when α or β changes. As the coherence time of pump laser is much greater than the path difference, $T_c \gg \Delta t$, the visibility of the fringes should be close to 1 since the two-photon state can be looked as an entangled state in infinity-dimension Hilbert space [25].

Figure 6(c) shows the experiment results of the quantum interference, in which a time domain filter of 60 ps (15 time bins) is applied to filter out the count in the center peak. The circles and squares are measured interference fringes of the coincidence counts when increasing α under fixed β of 3.41 or 4.83 rad, respectively, in which the accidental coincidence counts have been subtracted. The values of α and β are obtained according to the applied voltages on the two UMZIs. It can be seen that sinusoidal interference fringes appear when increasing α under the two fixed β values. The blue solid and red dashed lines are their fitting curves using sinusoidal functions. The visibilities of the two fringes are $92.3 \pm 1.20\%$ and $92.9 \pm 0.76\%$, respectively, without subtracting the accidental coincidence count. On the other hand, the single side count rates are almost unchanged during the measurement at both sides, showing that the fringes are the results of the quantum interference due to the energy-time entanglement.

Utilizing the measurement results shown in Fig. 6(c), a violation of Bell inequality [6, 20, 21] for the energy-time entanglement can be demonstrated. The Bell-inequality of the Clauser-Horne-Shimony-Holt (CHSH) form [6, 21] can be expressed as

$$S = |E(\alpha_1,\beta_1) + E(\alpha_1,\beta_2) + E(\alpha_2,\beta_1) - E(\alpha_2,\beta_2)| \leq 2 \tag{8}$$

where $E(\alpha_i,\beta_j),\ (i,j=1,2)$ is the correlation coefficient and α,β are the values of additional phases in the long arms of the two UMZIs. The interference fringes in Fig. 6(c) indicates that the coincidence count has a sinusoidal pattern depending on the total phase shifts $\alpha+\beta$, hence the correlation coefficient can be expressed as

$$E(\alpha,\beta) = V\cos(\alpha+\beta) \tag{9}$$

where V is the interference visibility.

According to the visibilities of the interference fringes shown in Fig. 6(c), the maximum value of CHSH-Bell inequality is $S_{\max} = 2\sqrt{2}V = 2.61 \pm 0.034$, a violation of Bell inequality of up to 18 standard deviations (σ) of the measurement uncertainty is presented, demonstrating the characteristics of energy-time entanglement in the photon-pairs generated in optical fibers via SFWM process under CW pumping.

4. Conclusion

In this paper, it is demonstrated that the photon-pairs generated by the SFWM in optical fibers under CW pumping can be used as the sources of energy-time entangled photon-pairs at 1.5 μm band, if the contributions of noise photons in coincidence counts is suppressed sufficiently by narrow time domain filter. In the experiment, the narrow time domain filter is realized by SNSPDs with low timing jitters and high time-resolution TCSPC module. Utilizing a time domain filter of 124 ps, experiment results show that although the generation rates of the noise photons at both sides are one order of magnitude higher than that of photon-pairs via SFWM, the coincidence count rates are always far higher than the accidental coincidence count rates with a maximum CAR of 15.8. The energy-time entanglement is demonstrated by an experiment of Franson-type interference. The interference visibilities under $\beta = 3.41$ rad and $\beta = 4.83$ rad are $92.3 \pm 1.20\%$ and $92.9 \pm 0.76\%$ (without subtracting the accidental coincidence count), respectively, in which the impact of accidental coincidence count is subtracted. These results indicate a violation of CHSH-Bell inequality of 18 standard deviations (σ) of the measurement uncertainty, presenting the energy-time entanglement property in the generated

#199979 - $15.00 USD Received 28 Oct 2013; revised 12 Dec 2013; accepted 17 Dec 2013; published 2 Jan 2014

photon-pairs. It shows that the SFWM in optical fibers under CW pumping provides a simple way to generate energy-time entangled photon-pairs at 1.5 μm, which would play an increasingly important role in long-distance quantum information applications over optical fibers.

Acknowledgments

This work was supported by 973 Programs of China under Contract No. 2011CBA00303 and 2010CB327606, China Postdoctoral Science Foundation, Tsinghua University Initiative Scientific Research Program, Basic Research Foundation of Tsinghua National Laboratory for Information Science and Technology (TNList), National Natural Science Foundation of China (91121022), Strategic Priority Research Program (B) of the Chinese Academy of Sciences (XDB04010200 and XDB04020100).

#199979 - $15.00 USD Received 28 Oct 2013; revised 12 Dec 2013; accepted 17 Dec 2013; published 2 Jan 2014